Accepted version: Andrew Chrysler, Cynthia Furse, Kaitlin Hall, Youchung Chung, "Effect of Material Properties on a Subdermal UHF RFID Antenna", *IEEE Journal of RFID*, 1(4), pp. 260-266, 2018

Effect of Material Properties on a Subdermal UHF RFID Antenna

Andrew Chrysler, *Student Member*, Cynthia Furse, *Fellow*, Kaitlin Hall, *Student Member*, Youchung Chung, *Senior Member*

***Abstract*— This paper explores a subdermal RFID antenna at 918 MHz. The antenna, made from ink encapsulated in thin sheets of biocompatible PET, is designed to be implanted in the fat layer just below the skin, with the muscle acting as a lossy ground plane. The antenna is a patch that uses a T-slot for matching. Three materials are tested – aluminum tape, ELCOAT ink, and inkjet printing. The effect of antenna conductivity and the properties of the fat/skin and muscle layers are explored. The ELCOAT ink performs very similar to the aluminum, but the inkjet printing creates a very thin layer that is subject to skin depth effects. This RFID antenna provides a good proxy for next generation work on subdermal antennas. It demonstrates that the fat layer can sufficiently insulate the antenna to enable subdermal applications, and that the muscle acts like a sufficient ground plane, but without the challenges of a PEC ground plane very near the antenna. The antenna could also be used on the skin surface if the impedance is properly tuned.**

Index Terms—Implantable Antennas, TattooAntennas, RFID, conductivity

I. Introduction

As personalized healthcare and miniaturized sensors enable monitoring and data acquisition of biological signals at the skin surface, passive RFID technology provides a battery-free telemetry option that links healthcare to the internet of things [1]. Some high frequency (HF) RFID (13.56 MHz) work in this area includes glucose monitoring [2], orthopedic implant identification [3], and aortic pressure sensors [4]. Passive ultrahigh frequency (UHF) (865-956MHz) RFID has recently been considered for implantable communication applications due its longer read distances. It is also low-cost, convenient in size, battery free, and able to be seamlessly integrated into real-time healthcare monitoring applications [5].

Epidermal RFID tags placed on the skin surface are part of a trend of wearable electronics [6]. These are called tattoo tags [7], and have found use as temperature sensors [8], strain sensors [9], and more. These and other RFID antennas have been manufactured at economies of scale using conductive ink, where the reduced conductivity of the ink produces mild reduction of antenna performance [7, 10-13]. When antennas are placed on the surface of the body, the body (particularly the highly conductive muscle) acts like a lossy ground plane and requires careful tuning of the antenna [14]. This is similar to the design of RFID antennas for placement on metal objects [15-17]. RFID tags have also been used extensively inside the body, particularly providing identification for pets and livestock, using very small coil antennas with limited range.

This paper describes a passive RFID antenna that is implanted just under the skin, injected or tattooed in the semi-insulating fat layer [18]. It builds on previous RFID experience in many ways while diverging in others. Unlike existing epidermal 'tattooed' antennas that are printed on plastic stickers that adhere to the more design flexibility than the tiny coils used for today's skin surface, the antenna in this paper is designed to be injectable below the skin, in the fat layer, more like a traditional tattoo. The materials used for this are antenna include inks and paints that could conceivably be injected under the skin. Current work in polymer engineering is underway to develop an injectable nanocomposite hydrogel that is initially a fluid but turns to a solid at body temperature,[19-21] and the materials used in this paper are good proxies for this up-and-coming new material. Subdermal antennas can be much larger, and have implantable RFID tags. Much existing RFID design experience with printed (imperfectly conducting) materials applies to the inherent imperfect conductivity of injectable materials. The design of RFID antennas over metal objects applies as well, as in our case, the muscle forms an imperfect, lossy ground plane for the antenna in the fat just above it.

This paper is an initial study of the effect of the various materials on the antenna performance--the imperfectly conducting injectable conductor making up the antenna, the imperfectly insulating fat that surrounds it, and the imperfectly conducting ground plane of the muscle below it. This work focuses on a fully implantable, subdermal UHF RFID antenna designed to cover the US (915MHz) and Korean (920MHz) RFID frequency bands. 918MHz is used for the simulations. This antenna uses an embedded T-match feed similar to [7, 22, 23]. Section II of this paper focuses on the effect of the material properties of the antenna by using two different inks that emulate injectable materials. The printed ink is very conductive (up to 2.22×10^7 S/m), but the skin depth exceeds the fabricated antenna thickness leading to losses. The other ink (ELCOAT) is less conductive (10^5 S/m) and thick enough that skin depth losses are negligible. Both inks provide insight into constraints that injected tattoo antennas will face. Section II also examines the effect of the material properties of the surrounding fat/skin (relatively low loss, acting as a sub and superstrate) and muscle (relatively high conductivity, acting as a lossy ground plane) [24-26]. Section III describes the fabrication and measurement of the antennas. Section IV describes how impedance tuning the T-slot can improve the match between the antenna and RFID chip.

II. Effect of Material Properties – Antenna Design and Simulation

This RFID antenna shown in Figure 1 is similar to the T-slot antenna from [7, 23]. It is designed for conjugate match with an Higgs 2 RFID IC strap manufactured by Alien [27] which has a

nominal complex impedance of 11.7 – 132jΩ at 918 MHz. To maximize read range [28], the antenna is tuned for maximum power transfer by adjusting the dimensions of the slot. The antenna is coated in a 0.1 mm PET envelope for biocompatibility and electrical insulation [29], has pointed ends to slightly improve the bandwidth, and is designed to operate in the fat layer under skin, as shown in Figure 2.

A. Effect of Antenna Conductivity

The conductive material the antenna is made of carries the surface current that produces the radiated fields, and is therefore critical to its performance and efficiency. Ideally, the highest conductivity material would be used. For an antenna that is injected or tattooed under the skin, there may be significant reduction in conductivity due to spreading out of the conductive material, incomplete connectivity due to surrounding biological material, etc. Reduction in conductivity alters the antenna performance, typically increasing its return loss, lowering the resonant frequency and increasing the bandwidth. Antennas with conductivities as low as 5 x 10^2 S/m have been proposed [30]. In this research, two different conductive inks were used as proxies for injectable biocompatible materials with similar conductivities. The first ink is ELCOAT, a thick paste made with conductive silver flakes that is easily painted to create the antenna shape. It has a conductivity of 10^5 S/m and can be spread with a thickness of approximately 100 µm. The second is silver ink that is inkjet printed by NovaCentrix [31]. This printing has a nominal thickness between 0.75 and 1 µm, and sheet conductivity between 60 and 70 mΩ/square, giving it a conductivity between 2.04 x 10^5 and 2.22 x 10^7 S/m. Although the ink is highly conductive, it is so thin that at 918 MHz the skin depth is larger than the ink thickness [32].

This RFID antenna is designed to operate underneath the skin, in the fat layer with muscle below. In the body the skin and the muscle are rather conductive, while the fat is somewhat insulating. This creates an environment that is electromagnetically similar to a microstrip antenna above a lossy ground plane. Table 1 summarizes the properties of the materials used in this work.

Table 1 Properties of materials at 918 MHz

Material	ε_r	σ [S/m]	Thickness	Skin Depth
Aluminum Tape		3.5 x 10^7	70 µm	2.8 µm
NovaCentrix [31]		2.04 x 10^5 --2.22 x 10^7	0.75 – 1 µm	3.52 - 36.7 µm
ELCOAT [33]		1 x 10^5	100 µm	52.5 µm
Muscle [24-26]	57.9	0.82	Simulation, 200 mm Measurement > 25 mm	18.3 mm
Skin [24-26]	46.7	0.68	0.062 mm	20.1 mm
Fat [24-26]	11.6	0.081	8.00 mm	58.4 mm

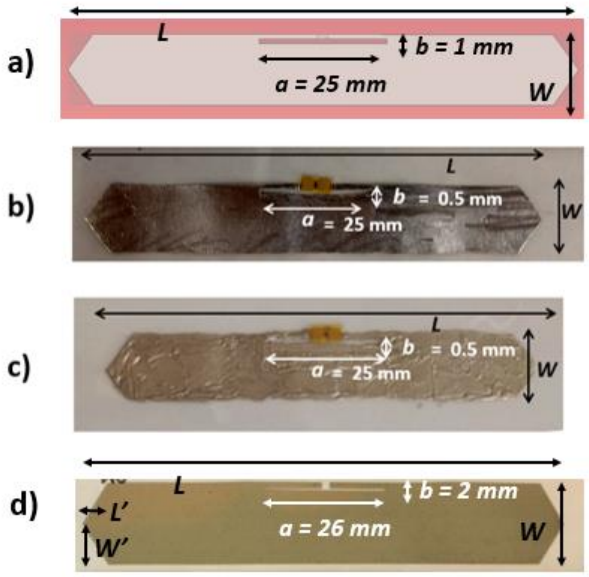

Fig. 1 Simulated and fabricated RFID antennas. The antennas are symmetric with L = 100 mm, L' = 5 mm, W = 15mm, and W' = 7.5 mm. a) Simulated antenna b) Aluminum tape (for comparison) c) ELCOAT conductive ink (painted) d) NovaCentrix inkjet printed

The antenna in Figure 1(a) was simulated in the skin-fat-muscle environment shown in Figure 2 using full wave simulation from CST. The antenna was excited by a 50 Ω discrete port, but its connection to the Higgs IC was simulated by calculating the S_{11} using (1), where Z_A is the antenna impedance, Z_{IC} is the chip impedance (=11.7 – 132jΩ) and Z_{IC}^* is its complex conjugate.

$$S_{11} = 20 \log_{10}\left(\frac{Z_A - Z_{IC}^*}{Z_A + Z_{IC}}\right) \quad (1)$$

The S_{11} was calculated as the conductivity of the antenna was varied from 10^2 to 10^7S/m, as shown in Figure 3 and summarized in Table 2. When the conductivity is above 10^5 S/m, the antenna performs very similar to if it is copper. Between 10^2 and 10^5 S/m the performance degrades significantly. As the conductivity decreases the resonant frequency decreases, the bandwidth increases (as expected from [34]), and the return loss increases.

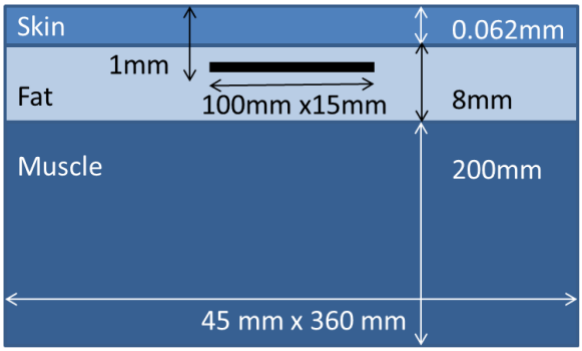

Fig. 2 Simulation model of the RFID antenna shown in Figure 1, embedded in the fat layer. The antenna (0.07mm thick) is coated with 0.1mm of insulating PET. The bottom of the coated antenna is 1mm below the surface of the skin.

Table 2: Simulated effect of antenna conductivity on S_{11}, resonant frequency and bandwidth. The slot size is a = 25 mm and b = 1 mm, and S11 is calculated assuming it is connected to a Higgs 2 chip with Z = 11.7 – 132jΩ.

Conductivity [S/m]	Resonant Frequency [MHz]	S_{11} [dB]	3 dB Bandwidth [%]
10^2	563	-2.51	--
10^3	768	-3.11	7.3
10^4	868	-5.02	16.0
10^5	902	-7.53	15.2
5.8 x 10^7 (Copper)	917	-10.45	13.7

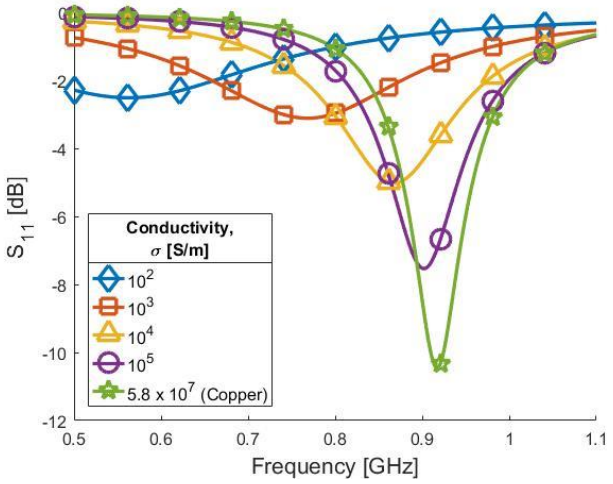

Fig. 3. Simulated S_{11} of antenna in Figure 1(a) in the environment shown in Figure 2 as the conductivity of the antenna is varied. The simulated antenna is assumed to be excited by a Higgs 2 IC. As the conductivity decreases, the S_{11} deteriorates, the resonant frequency decreases, and the bandwidth increases. Antennas with conductivity as low as 10^2 S/m may be useful in some applications.

B. Effect of Fat andMuscle

To examine the effect the biological tissues play in antenna performance, three simulations were performed and compared to the initial simulation environment shown in Figure 2. First, the PEC antenna was moved to the skin surface rather than being imbedded in the fat. The S_{11} for this case is similar to the initial simulation with the antenna imbedded in the fat, but the center frequency is shifted upwards from 918 MHz to 1.31 GHz. At 1.31 GHz the antenna impedance is 9.53 + j91.8 Ω. This detuning is caused by two things -- the additional separation between the antenna and muscle and the radiated fields being in air rather than partly in fat. The T-junction could be used to re-tune the antenna and bring the resonant frequency back to the desired band.

A second experiment was moving the antenna to the junction between the fat and muscle. In this case, the center frequency remains constant, but the S_{11} is reduced to -2.0 dB. This is caused by closer contact with the more lossy muscle. When the antenna is placed on the muscle, the impedance at 918 MHz resonance is 61.9 + j 83.7 Ω. Recall that this antenna does not directly short out against the muscle because of the plastic coating. A third experiment was to change the properties of the muscle to those of PEC with the PEC antenna imbedded in its original position in the fat layer. The center frequency is shifted slightly upwards from 918 MHz to 944 MHz, but the S_{11} is greatly improved to -40.5 dB and the impedance is 10.9 + j 128.9 Ω. From these simulations, it becomes clear that the muscle is acting as a ground plane, albeit a lossy ground, for the antenna and that the deep implantation of the RFID tag can result in significant reduction in antenna performance. Placing the antenna directly on muscle greatly increases the real impedance, which detunes the antenna significantly. When the antenna is placed on skin or the muscle properties are changed to PEC the real impedance is close to 10 Ω which improves the return loss.

III. Fabrication and Measurement

To validate the simulations from Section II, antennas shown in Figure 1(b-d) were fabricated and tested. The antenna in Figure 1(b) was fabricated using aluminum foil tape (σ = 3.5 x 10^7 S/m, thickness of 0.07 mm) cut by hand and affixed to a PET lamination film 0.1mm thick. The aluminum was used simply to have a comparison between the inks and a highly conductive, solid antenna. It was not considered as a viable biocompatible option. The antenna in Figure 1(c) was fabricated using ELCOAT conductive paste (σ = 1 x 10^5 S/m, thickness approximately 0.1 mm [33]). Thickness was determined using a caliper accurate to 0.01mm. The ELCOAT paste was applied using a template onto the PET lamination film. The antenna in Figure 1 (d) was inkjet printed by NovaCentrix (σ approximately 2 x 10^5 – 2 x 10^7 , thickness approximately 0.75 – 1 µm [31]). Each antenna was designed for a center frequency of 918 MHz by simulating the material using the properties in Table 1 and adjusting the slot size (a and b seen in Figure 1) to give the best S_{11} at 918 Mhz. These tuned slot dimensions given in the figure. The CST simulation results for S_{11} for the aluminum and ELCOAT antennas are shown in Figure 6. After each antenna was laid out onto the lamination film, a Higgs 2 RFID chip was placed across the terminal gap and affixed using ELCOAT paste. The functionality of the chip was verified using a handheld reader, and then the antenna assembly was passed through a laminating machine. The lamination process heats the PET film and affixes the antenna between the sheets creating a fully sealed, biocompatible envelope less than 0.3mm thick.

The biological environment was approximated during measurement by placing the antenna on top of a block of pork loin meat (approximating muscle) at room temperature. The pork was approximately 60x120mm and 40 mm thick. A thin slice (approximately 2mm thick) of deli meat (containing more fat than the pork) was placed on top of the antenna to simulate the effect of the fat and skin as seen in Figure 4.

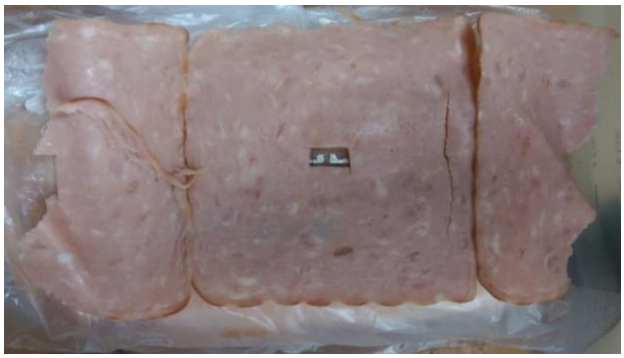

Fig. 4. RFID antenna S_{11} measurement set up. The ELCOAT RFID is on block of pork meat and covered by deli meat approximately 2 mm thick. There is a small window for measurement using a two-prong probe.

The return loss of the antenna at 918 MHz was measured with an Agilent E5071B Vector Network Analyzer. To connect the antenna to the analyzer, a two-prong probe was built that could be held across the gap where the Higgs 2 strap would be placed during RFID operation. The probe was made from a piece of semi-rigid coax with the inner conductor protruding to act as one part of the probe, and a piece of wire soldered to the external rigid shield to act as the other probe. A comparison of the simulated and measured S_{11} of the antennas is shown in Figure 6. The ELCOAT and aluminum antennas are very similar, indicating that ELCOAT is sufficiently conductive to be used for this type of antenna development. A simulated PEC antenna is shown for comparison, although it should be noted that the properties used for the biological materials (Table 1) may not be exactly the same as those used for measurement. The NovaCentrix inkjet printed antenna is thinner than the skin depth, so we adjusted the conductivity of the simulated antenna until it performed approximately the same as the NovaCentrix antenna. This gives an approximate effective conductivity of 10^3 S/m for the inkjet printed antenna.

As discussed in Section II, the antenna is designed to have a large inductance and small resistance at 918 MHz in order to create a complex conjugate impedance match to a Higgs 2 IC ($Z=11.7 - 132j\Omega$). The impedance of each antenna and its resonant frequency is given in Table 3. The NovaCentrix and the low conductivity metal have different slot sizes, but both have very large resistance at the design frequency. The other high impedance antennas have lower resistance, and the PEC antenna has the lowest resistance. All antennas have a large inductive component. As seen in Table 3, the slot dimensions can be readily adjusted to match the imaginary part of the impedance quite well, regardless of the material used. The real part of the impedance is more difficult to control. The lower loss materials (e.g. PEC) have lower real part of the impedance, which better matches the RFID chip. Thus, methods that improve the real part of the match would be beneficial for higher loss materials. Also, the frequency for each antenna can be adjusted by changing the overall size of the antenna, which was not done in this paper, because we wanted to compare antennas of exactly the same size.

Table 3. Impedance of simulated and RFID antennas shown in Figure 1. These antennas were designed to conjugate match to a Higgs 2 RFID IC ($Z=11.7 - 132j\Omega$). Antennas were measured on pork as described above.

Antenna	Slot Size (a x b) [mm]	Impedance [Ω]	Resonant Frequency [MHz]
PEC Simulation	25 x 1.0	21.2 + j130	918
Low Conductivity (10^3 S/m) Simulation	21 x 0.5	68.4 + j126	889
Aluminum Tape Measured	25 x 0.5	32.6 + j126.2	905
ELCOAT Ink Measured	25 x 0.5	35.5 + j124.0	915
NovaCentrix Measured	26 x 2.0	62.8 + j100.7	900

The read range of the RFID tags was measured in a hallway in the engineering building at Daegu University to approximate a rich multipath environment as seen in Figure 5. An Alien 9800 reader at 1 W was connected to two 6 dBi antennas to read the RFID antenna. The antenna was placed in the pork/deli meat proxy for the body and slowly moved toward the reader antennas until a positive read was verified. Maximum average read range was 109 cm for the aluminum antenna and 101cm for the ELCOAT antenna. The NovaCentrix inkjet printed antenna was not tested for read range.

Fig. 5. RFID read distance measurement setup in a multipath environment of a hallway in the engineering building at Daegu University.

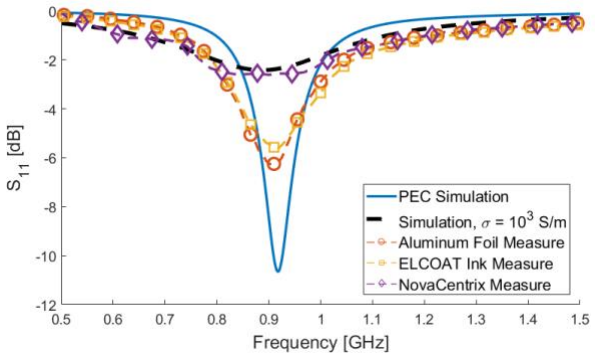

Fig. 6 Comparison of S_{11} for the RFID antennas shown in Figure 1 when matched to a Higgs 2 chip. The ELCOAT and aluminum antenna behave very similarly. The NovaCentrix antenna behaved similar to a simulated antenna with $\sigma=10^3$ S/m.

IV. T-SLOT MATCHING

The dimensions of the slot are important to the operation of this antenna and may be tuned to improve performance. The NovaCentrix inkjet printed antenna was used for this experiment, because it has the best ability to precisely control slot size. Figures 7-10 show the real and imaginary impedance variance and S_{11} for several slot dimensions.

First, the antenna impedance is tuned by keeping slot length, *a*, constant at 25 mm while the width, *b*, is varied from 0.5 – 2.5 mm. As seen in Figures 7 and 8, as the slot width, *b*, increases the measured impedance and reactance of the antenna increases greatly. Decreasing slot width, *b*, increases the center frequency of the S_{11}. This effect is expected based on [7]. Next, the antenna impedance is tuned by keeping slot width, *b*, constant at 0.5 mm and the length, *a*, is varied from 20-30 mm. As seen in Figures 9 and 10, the real impedance is not affected as strongly as the reactance. Decreasing the slot length, *a*, increases the S_{11} center frequency. At the 918 MHz design frequency the slot length, *a*, appears to have less effect on the antenna tuning than the slot width, *b*. Again, this effect is also expected based on [7].

As the slot dimensions are closely related to antenna performance it is expected that there should be a considerable current distribution around the slot. Figure 11 shows the high current density around the slot during several phases of the wave. Both the pointed edges and the bottom of the antenna have low current distributions indicating that these portions of the antenna could be removed or reduced if desired. When considering injectable antennas, these current distributions indicate that larger conductivity is needed near the feed/slot, and lower conductivity could be used further from the slot.

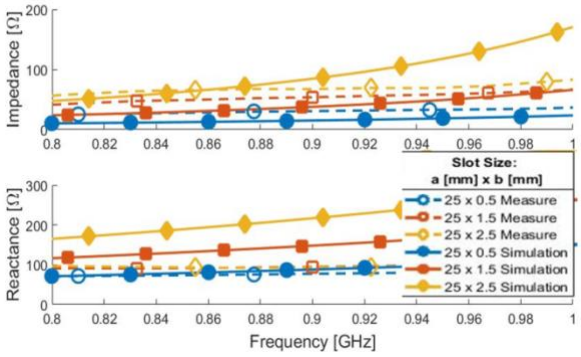

Fig. 7. Impedance of the NovaCentrix RFID antenna as slot length, *a*, is kept constant at 25 mm and the width, *b*, is varied from 0.5 – 1.5 mm

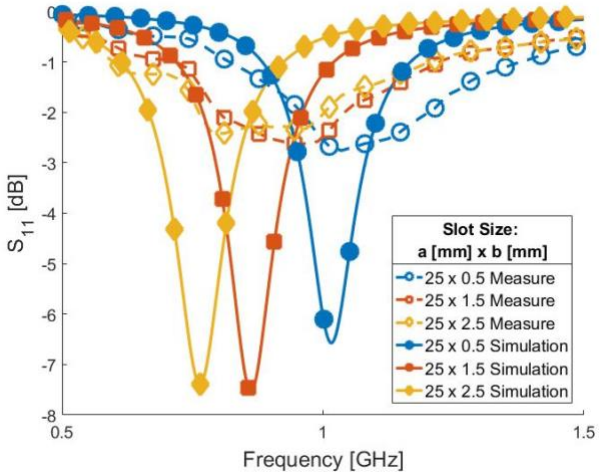

Fig. 8. S_{11} of the NovaCentrix inkjet printed antenna as slot length, *a*, is kept constant at 25 mm and the width, *b*, is varied from 0.5 – 1.5 mm

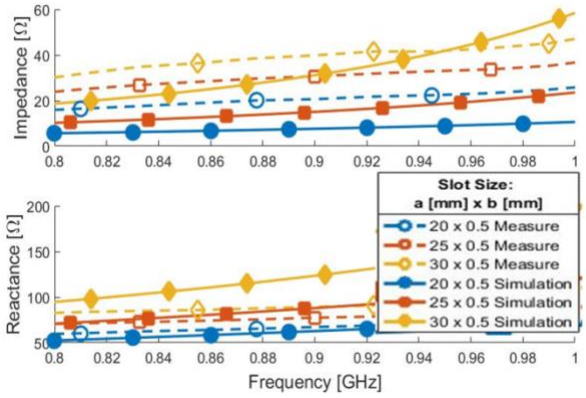

Fig. 9. Impedance of the NovaCentrix RFID antenna as slot width, *b*, is kept constant at 0.5 mm and the length, *a*, is varied from 20-30 mm.

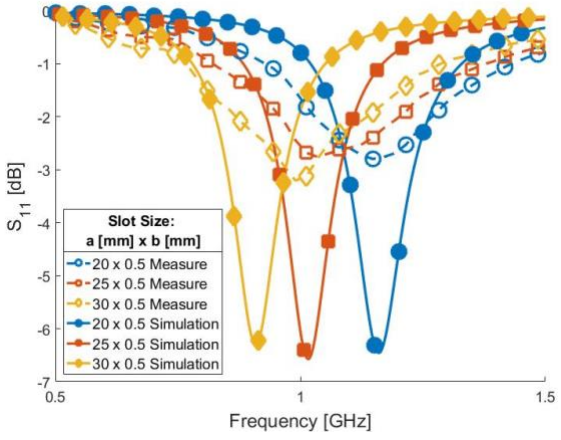

Fig. 10. S_{11} of the NovaCentrix inkjet printed RFID antenna as slot width, *b*, is kept constant at 0.5 mm and the length, *a*, is varied from 20-30 mm.

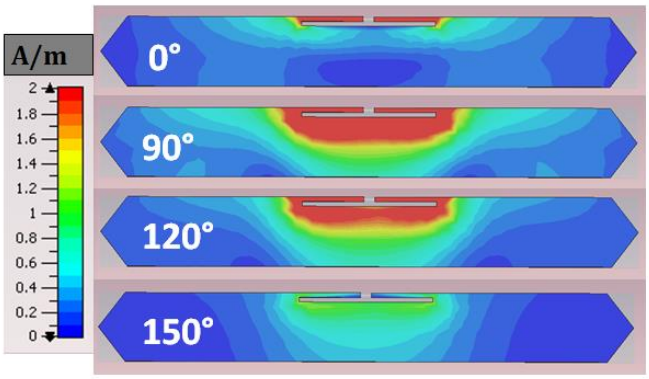

Fig. 11. Simulated current distribution in the PEC RFID antenna at 918 MHz. The current is strongest near the slot and weaker away from it.

V. Conclusions & Future Work

A subdermal RFID antenna made from conductive ink is presented here. The materials used here are proxies for biocompatible inks that could be injected in the fat layer below the skin, with muscle below. The fat acts like a semi-insulator for the antenna and the muscle as a lossy ground plane, creating an environment that is electromagnetically similar to a microstrip antenna above a lossy ground plane.

The effect of the conductivity of the antenna is considered using aluminum tape and two different types of conductive ink. The first ink, ELCOAT, has a conductivity of 10^5 S/m and performs nearly as well as an antenna made from aluminum tape. Both have a read distance using an Alien 1W RFID reader at 918 MHz of greater than 100 cm. The second antenna is made by NovaCentrix and is very conductive (up to 10^7 S/m) but suffers from skin effect losses. The skin effect losses cause the antenna to behave similar to an antenna with a conductivity in the range of 10^3 S/m. Simulations show that antennas with conductivity as low as 10^2 may be useful in some applications. The slot dimensions can be used to tune the impedance of the antenna, as demonstrated using the NovaCentrix inkjet printed antennas.

This RFID antenna provides a good proxy for next generation work on subdermal antennas. It demonstrates that the fat layer can sufficiently insulate the antenna to enable subdermal applications, and that the muscle acts like a sufficient ground plane. An antenna injected in the fat this way acts very similar to an antenna on the skin surface, thus making it possible to utilize the experience with epidermal RFID tags to design subdermal tags as well, with some retuning via the slot.

Acknowledgement

The authors wish to acknowledge the National Science Foundation for funding this work through grant number 1310642 and the East Asia Pacific Summer Institute (EAPSI) program.

References

[1] S. Amendola, R. Lodato, S. Manzari, C. Occhiuzzi, and G. Marrocco, "RFID Technology for IoT-Based Personal Healthcare in Smart Spaces," *IEEE Internet of Things Journal*, vol. 1, no. 2, pp. 144-152, 2014.

[2] Z. Xiao *et al.*, "An Implantable RFID Sensor Tag toward Continuous Glucose Monitoring," *IEEE Journal of Biomedical and Health Informatics*, vol. 19, no. 3, pp. 910-919, 2015.

[3] X. Liu, J. L. Berger, A. Ogirala, and M. H. Mickle, "A Touch Probe Method of Operating an Implantable RFID Tag for Orthopedic Implant Identification," *IEEE Transactions on Biomedical Circuits and Systems*, vol. 7, no. 3, pp. 236-242, 2013.

[4] O. Romain *et al.*, "RFID implantable pressure sensor for the follow-up of abdominal aortic aneurysm stented," in *2011 6th International Conference on Design & Technology of Integrated Systems in Nanoscale Era (DTIS)*, 2011, pp. 1-6.

[5] G. Marrocco, "Body-matched RFID antennas for wireless biometry," in *2006 First European Conference on Antennas and Propagation*, 2006, pp. 1-5.

[6] D.-H. Kim *et al.*, "Epidermal electronics," *science*, vol. 333, no. 6044, pp. 838-843, 2011.

[7] M. A. Ziai and J. C. Batchelor, "Temporary On-Skin Passive UHF RFID Transfer Tag," *IEEE Transactions on Antennas and Propagation*, vol. 59, no. 10, pp. 3565-3571, 2011.

[8] S. Milici, S. Amendola, A. Bianco, and G. Marrocco, "Epidermal RFID passive sensor for body temperature measurements," in *2014 IEEE RFID Technology and Applications Conference (RFID-TA)*, 2014, pp. 140-144.

[9] O. O. Rakibet, C. V. Rumens, J. C. Batchelor, and S. J. Holder, "Epidermal Passive RFID Strain Sensor for Assisted Technologies," *IEEE Antennas and Wireless Propagation Letters*, vol. 13, pp. 814-817, 2014.

[10] G. A. Casula, G. Montisci, and G. Mazzarella, "A Wideband PET Inkjet-Printed Antenna for UHF RFID," *IEEE Antennas and Wireless Propagation Letters*, vol. 12, pp. 1400-1403, 2013.

[11] A. Chrysler, C. Furse, and Y. Chung, "Biocompatible, implantable UHF RFID antenna made from conductive ink," in *2016 IEEE International Symposium on Antennas and Propagation (APSURSI)*, 2016, pp. 467-468.

[12] D. Bechevet, V. Tan-Phu, and S. Tedjini, "Design and measurements of antennas for RFID, made by conductive ink on plastics," in *2005 IEEE Antennas and Propagation Society International Symposium*, 2005, vol. 2B, pp. 345-348 vol. 2B.

[13] J. Siden and H. E. Nilsson, "Line width limitations of flexographic-screen- and inkjet printed RFID antennas," in *2007 IEEE Antennas and Propagation Society International Symposium*, 2007, pp. 1745-1748.

[14] S. Amendola, S. Milici, and G. Marrocco, "Performance of Epidermal RFID Dual-loop Tag and On-Skin Retuning," *IEEE Transactions on Antennas*

and Propagation, vol. 63, no. 8, pp. 3672-3680, 2015.

[15] S. Genovesi and A. Monorchio, "Low-Profile Three-Arm Folded Dipole Antenna for UHF Band RFID Tags Mountable on Metallic Objects," *IEEE Antennas and Wireless Propagation Letters*, vol. 9, pp. 1225-1228, 2010.

[16] H. Kwon and B. Lee, "Compact slotted planar inverted-F RFID tag mountable on metallic objects," *Electronics Letters*, vol. 41, no. 24, pp. 1308-1310, 2005.

[17] L. Ukkonen, L. Sydanheimo, and M. Kivikoski, "Patch antenna with EBG ground plane and two-layer substrate for passive RFID of metallic objects," in *IEEE Antennas and Propagation Society Symposium, 2004.*, 2004, vol. 1, pp. 93-96 Vol.1.

[18] A. Chrysler, C. Furse, and Y. Chung, "Biocompatible, implantable UHF RFID antenna made from conductive ink," in *Antennas and Propagation (APSURSI), 2016 IEEE International Symposium on*, 2016, pp. 467-468: IEEE.

[19] B. Yao *et al.*, "Ultrahigh‐Conductivity Polymer Hydrogels with Arbitrary Structures," *Advanced Materials*, 2017.

[20] G. Chen, F. Svec, and D. R. Knapp, "Light-actuated high pressure-resisting microvalve for on-chip flow control based on thermo-responsive nanostructured polymer," *Lab on a Chip*, vol. 8, no. 7, pp. 1198-1204, 2008.

[21] N. S. Satarkar, W. Zhang, R. E. Eitel, and J. Z. Hilt, "Magnetic hydrogel nanocomposites as remote controlled microfluidic valves," *Lab on a Chip*, vol. 9, no. 12, pp. 1773-1779, 2009.

[22] G. Marrocco, "RFID Antennas for the UHF Remote Monitoring of Human Subjects," *IEEE Transactions on Antennas and Propagation*, vol. 55, no. 6, pp. 1862-1870, 2007.

[23] G. Marrocco, "The art of UHF RFID antenna design: impedance-matching and size-reduction techniques," *IEEE Antennas and Propagation Magazine*, vol. 50, no. 1, pp. 66-79, 2008.

[24] C. Gabriel, S. Gabriel, and E. Corthout, "The dielectric properties of biological tissues: I. Literature survey," *Physics in medicine and biology*, vol. 41, no. 11, p. 2231, 1996.

[25] S. Gabriel, R. W. Lau, and C. Gabriel, "The dielectric properties of biological tissues: III. Parametric models for the dielectric spectrum of tissues," *Physics in medicine and biology*, vol. 41, no. 11, p. 2271, 1996.

[26] S. Gabriel, R. W. Lau, and C. Gabriel, "The dielectric properties of biological tissues: II. Measurements in the frequency range 10 Hz to 20 GHz," *Physics in medicine and biology*, vol. 41, no. 11, p. 2251, 1996.

[27] *Higgs 2 Data Sheet*. Available: http://www.rfidusa.com/Pdf/Specials/Alien-DS_Higgs-2_EPC_Class_1.pdf

[28] K. V. S. Rao, P. V. Nikitin, and S. F. Lam, "Antenna design for UHF RFID tags: a review and a practical application," *IEEE Transactions on Antennas and Propagation*, vol. 53, no. 12, pp. 3870-3876, 2005.

[29] H. Seitz, S. Marlovits, I. Schwendenwein, E. Müller, and V. Vécsei, "Biocompatibility of polyethylene terephthalate (Trevira® hochfest) augmentation device in repair of the anterior cruciate ligament," *Biomaterials*, vol. 19, no. 1-3, pp. 189-196, 1998.

[30] C. D. Rouse, M. R. Kurz, B. R. Petersen, and B. G. Colpitts, "Performance Evaluation of Conductive-Paper Dipole Antennas," *IEEE Transactions on Antennas and Propagation*, vol. 61, no. 3, pp. 1427-1430, 2013.

[31] *NovaCentrix Web Page*. Available: https://www.novacentrix.com/

[32] J. R. Saberin and C. Furse, "Challenges with Optically Transparent Patch Antennas," *IEEE Antennas and Propagation Magazine*, vol. 54, no. 3, pp. 10-16, 2012.

[33] *ELCOAT Ink Purchase Site*. Available: http://www.hanatechno.com/front/php/product.php?product_no=377&main_cate_no=86&display_group=1

[34] M. Shahpari and D. V. Thiel, "The Impact of Reduced Conductivity on the Performance of Wire Antennas," *IEEE Transactions on Antennas and Propagation*, vol. 63, no. 11, pp. 4686-4692, 2015.